batteries

MDPI

Article

A Modified Acrylic Binder Used for the Graphite Negative Electrode in LithiumIon Batteries

Lianxiang Feng, Wenting Chen, Feng Hai, Xin Gao, Yuyu Ban, Weicheng Xue, Wentao Yan, Yunxiao Yang and Mingtao Li *

Shaanxi Key Laboratory of Energy Chemical Process Intensification, School of Chemical Engineering and Technology, Xi'an Jiaotong University, No. 28, Xianning West Road, Xi'an 710049, China; 4521216003@stu.xjtu.edu.cn (L.F.); loveney@stu.xjtu.edu.cn (W.C.); mrhaifeng.1009@stu.xjtu.edu.cn (F.H.); gaoxin1477@stu.xjtu.edu.cn (X.G.); 3123134024@stu.xjtu.edu.cn (Y.B.); xwc991012@stu.xjtu.edu.cn (W.X.); yanwentao@stu.xjtu.edu.cn (W.Y.); yunx2002@stu.xjtu.edu.cn (Y.Y.)
* Correspondence: lmt01558@mail.xjtu.edu.cn

Abstract: The water-based binder has the advantages of non-toxic, non-flammable, small odor, and no pollution to the environment. However, there are problems such as low bond strength and poor battery cycle life of commonly used binders on the market. In this paper, the acrylic binder is modified. In addition, acrylic acid/methacrylic acid, acrylonitrile, and octadecyl acrylate/octadecyl methacrylate are copolymerized at high temperature, and a new binder for graphite anode is successfully developed. The binder can significantly improve the affinity between the graphite anode and the electrolyte and the integrity of the graphite particles during the cycle, so that the battery has better electrochemical performance. During the charge and discharge cycle of 1 C, the graphite anode coated with PAANa as a binder was able to cycle 360 cycles and remain stable, which is far better than the 192 cycles of the commercial binder LA133. It is proved that the experimental formula has a certain commercial application prospect.

Keywords: binder; lithium metal batteries; graphite

Academic Editor: Dino Tonti

Received: 25 December 2024
Revised: 28 April 2025
Accepted: 1 May 2025
Published: 13 May 2025

Citation: Feng, L.; Chen, W.; Hai, F.; Gao, X.; Ban, Y.; Xue, W.; Yan, W.; Yang, Y.; Li, M. A Modified Acrylic Binder Used for the Graphite Negative Electrode in LithiumIon Batteries. *Batteries* **2025**, *11*, 190. https://doi.org/10.3390/batteries11050190

1. Introduction

The lithium-ion battery (LIB), as an important secondary battery energy storage device, has become the power source of electric vehicles because of its high energy density, light weight, no self-discharge phenomenon, and excellent cycle performance [1–3]. After years of technological accumulation, electric vehicles have gradually entered the mass market in recent years [4,5]. However, the continuous development of the electric vehicle industry has put forward higher requirements for driving range, and it is necessary to modify the existing positive and negative electrode materials, electrolytes, or binders [6,7].

In the electrode of LIB, the binder is an important component. It not only plays a role in binding the active material, conductive agent, and current collector, but it also plays an important role in maintaining electrode integrity and constructing ion and electron transport channels [8–10]. In addition to having good bonding ability, a good binder should also have good mechanical properties and machinability under the condition of low binder content, especially in terms of flexibility and viscosity [11,12]. Graphite is the most widely used anode material for lithium-ion batteries. In the process of charging and discharging, lithium ions are repeatedly embedded and removed between graphite layers, and the graphite is prone to rupture and fall off, which affects the comprehensive performance and

service life of the battery [13,14]. Therefore, it is very important to find a suitable graphite negative binder.

Graphite electrodes are usually manufactured with water-based binders, such as Carboxymethyl Cellulose (CMC), Polymerized Styrene, Butadiene Rubber (SBR), polyacrylate binders LA133, and so on. The volume of negative electrode materials, such as graphite, changes greatly during the charge and discharge process. Water-based binders can better adapt to this change by preventing the fragmentation and displacement of active material particles, thereby maintaining the stability of the electrode [15]. The stability of CMC slurry as a binder is poor, and the chemical gelling phenomenon easily to occurs [16]. Wirth SBR, it is easy to break the latex under long stirring, so as to damage the structure and reduce its cohesiveness [17–19]. LA133 used in the process requires attention in order to adjust the viscosity of the paste, and the drying temperature of the pole film during the coating process should not be too high, otherwise it is prone to curling or coating cracking [20]. In this case, there is an urgent need for new binders with excellent comprehensive properties to further improve battery performance.

In our work, acrylic acid/methacrylic acid, the acrylonitrile with cyanide group, which is beneficial to form hydrogen bond and strengthen bonding property, and the addition of long chain octadecyl acrylate/octadecyl methacrylate in the LA133 structure, which is conducive to the flexibility of the binder, are used as raw materials to prepare the binder PAANa. In the reaction process of raw materials, ammonium persulfate/potassium persulfate/sodium persulfate/hydrogen peroxide is used as an initiator to accelerate the reaction. The experimentally synthesized binder and the commercial binder LA133 were, respectively, used to make graphite electrode sheets. Through the comparison of battery cycles, it can be found that PAANa has better cycle life and rate performance. The feasibility of the experimental formulation is proved, which provides a reference direction for developing better commercial binders.

2. Materials and Methods

2.1. Materials

Acrylic acid (AA, 99%), Acrylonitrile (AN, 99%), Stearyl Acrylate (SA, 96%), Ammonium persulfate (APS, 98%), and Sodium hydroxide (NaOH, 96%) are purchased from Aladdin.

2.2. Synthesis Methode of the PAANa

In the reactor, 4 L of deionized water, 0.8 kg of acrylic acid, 0.3 kg of acrylonitrile, and 0.2 g of stearyl acrylate or stearyl methacrylate were added and homogenized thoroughly. The temperature was then elevated to 70 °C, followed by the addition of an initiator solution (3 g of ammonium persulfate dissolved in 0.1 L of water) via dropwise addition over approximately 2 h, during which the temperature was maintained at 70 °C. After complete addition, the reaction temperature was increased to 75 °C and maintained for 2 h. Subsequently, the temperature was further raised to 80 °C, and an additional initiator solution (1 g of ammonium persulfate dissolved in 0.1 L of water) was introduced. The mixture was held at this temperature for 1 h to ensure thorough monomer consumption. Upon completion of the reaction, the system was cooled to 50 °C and neutralized to pH 8.0 using 1.25 kg of aqueous sodium hydroxide solution (30% w/w). The solid content was determined, and deionized water was added to adjust the final solid content to 15%. The product was then cooled to 30 °C and filtered through a 200-mesh steel wire filter.

2.3. Characterization of PAANa

Fourier transform infrared spectrometer (FT-IR, Bruker VERTEX70, Xi'an, China) was used to test with a wave number of 1000–4000 cm^{-1}, and the test mode was selected as attenuated total reflection (ATR). The thermogravimetric curves were obtained using a simultaneous thermal analyzer (NETZSCH-STA449F5, Xi'an, China) in a nitrogen atmosphere at a ramp rate of 10 °C min^{-1} from room temperature to 500 °C. The structural composition of cycled graphite cathode was evaluated by X-ray photoelectron spectroscopy (XPS, K-ALPHA, Shanghai, China). Time of Flight Secondary Ion Mass Spectrometer (ToF-SIMS, M6, Shanghai, China) was used to observe the surface composition of the lithium metal after the cycle.

2.4. Lithium Battery Manufacturing and Performance

High-rate graphite (Canrd, ref. MA-EN-AN-001601) (80 wt%), carbon black (10 wt%) and LA133 (10 wt%) were mixed well and then stirred with appropriate amount of deionized water dropwise. Subsequently, the slurry was coated on aluminum foil and dried in a vacuum oven at 50 °C for 12 h. The binder PAANa was used to prepare the graphite anode in the same way. Coin-type cells were assembled using graphite cathode (load 2.2~2.5 mg), electrolyte KLD-1230C and lithium metal anode (diameter 16 mm) in sequence. The cell was then left at room temperature for 6 h so that the electrolyte completely wets the interface. All the operations were carried out in an argon-filled glove box (H_2O < 0.1 ppm, O_2 < 0.1 ppm). Constant-current charge/discharge and cycling performance were tested at 25 °C using a battery test system (Neware Electronic Co., Ltd. Shenzhen, China) at 0.1 to 2 V potential. The surface morphology of graphite cathode before and after cycling was observed using a field emission scanning electron microscope (FESEM, MAIA3 LMH equipped with energy dispersive X-ray spectroscopy (EDS), Shanghai, China). Cyclic voltammetry (CV) tests were performed with a scan rate of 0.5 mV s^{-1} between 0.1 and 2 V.

3. Results

The molecular structure of PAANa is shown in Figure 1a. The two binder solutions are dried at 50 °C for 5 h, and then placed in a vacuum oven at 110 °C for 12 h, and the water is completely removed to obtain solid samples. The samples are, respectively, tested by FT-IR (wavelength 1000–4000 cm^{-1}), and the results are shown in Figure 1b. The characteristic peak of C=C does not appear in the curve of PAANa, but the characteristic peak of C≡N appears at 2250 cm^{-1}, and the characteristic peak of C=O appears at 1660 cm^{-1}. It shows that all monomers reacted and the required binder was obtained by successful copolymerization.

Thermogravimetric tests are performed on PAANa and LA133 in a nitrogen atmosphere with a temperature increase rate of 10 °C min^{-1} and within a temperature range of 30 °C~500 °C. The thermogravimetric curves in Figure 1c show that both PAANa and LA133 are decomposed in one step. However, it is obvious that the decomposition temperature of PAANa is higher than LA133, indicating that PAANa has better thermal stability.

The experimental binder PAANa and commercial binder LA133 were mixed with graphite and carbon black, respectively. After drying, the mechanical properties of the two binders were tested by a tensile machine. The two pole pieces to cut to the same size and then taped separately. The two clamps of the tension machine were, respectively, held in the pole piece and the adhesive cloth and the program was set up to test the adhesion strength of the binder. The results were shown in Figure 1d. The average adhesion strength of PAANa was 2.8 N, while the average peeling strength of LA133 was only 1.95 N. Through comparison, it is obvious that the adhesion strength of PAANa is larger, indicating that it has better bonding property.

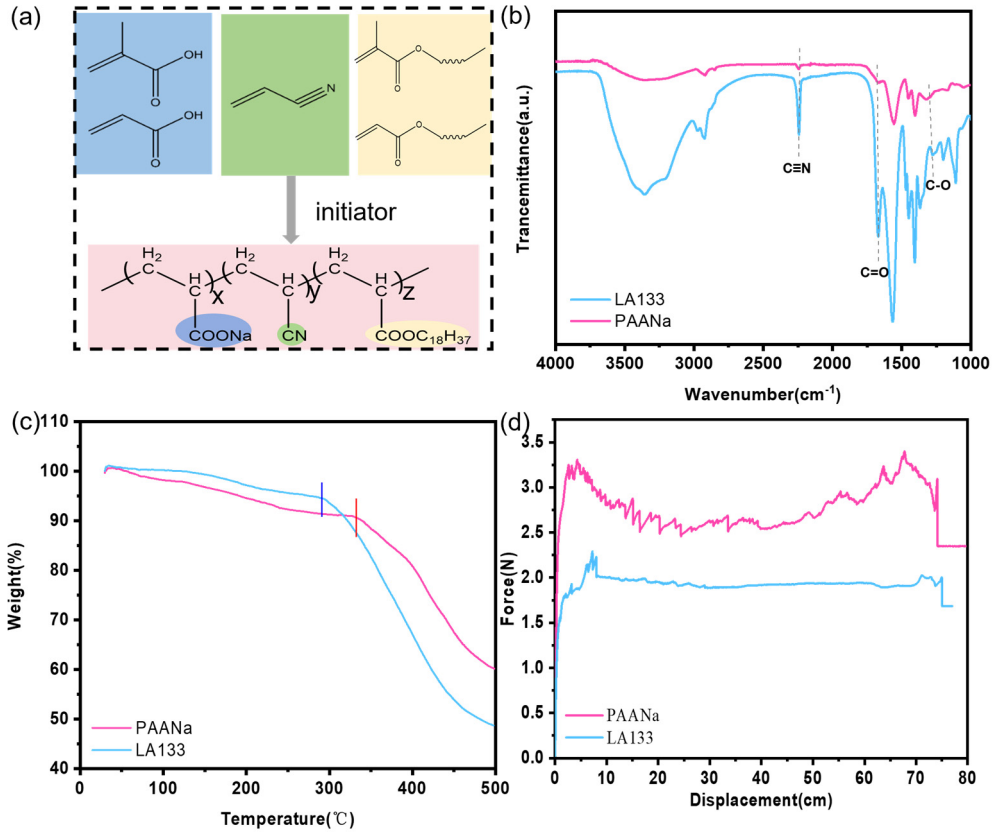

Figure 1. (**a**) Molecular structure of PAANa. (**b**) FT-IR, (**c**) TGA, and (**d**) Tensile test of PAANa and LA133.

Cyclic voltammetry curves of graphite negative electrodes with different binders were tested at 0.1 mV s^{-1} sweep speed, and the results were shown in Figure 2a,b. It can be found that the two binders have an oxidation peak and a reduction peak, corresponding to the removal and embedding of Li+ in the graphite layer, respectively. The comparison shows that PAANa not only has a higher current density but also a smaller battery polarization. The better CV curve performance of PAANa binder is related to the higher adhesion strength, which is more conducive to the good contact between the active substance and the conductive agent and the integrity of the electrode. After 180 cycles of the battery, the current density of both PAANa and LA133 decreased, and the voltage difference in the REDOX peak increased slightly. This is because side reactions on the electrode surface (such as electrolyte decomposition) accumulate SEI passivation layers. The analysis shows that using PAANa as a binder, the battery would have faster kinetics and better electrochemical performance.

Graphite sheets made of two kinds of binders are assembled into coin batteries and their electrochemical properties are tested. It can be observed from Figure 2c that the specific discharge capacity of PAANa is as high as 346 mAh g^{-1} after stabilization, while that of LA133 is only 335 mAh g^{-1} after stabilization. Using CMC as a binder can allow stability to be reached faster than PAANa and LA133. However, the capacity is smaller than PAANa and comparable to LA133. LA133 capacity decreased after 190 cycles, CMC capacity decreased after 200 cycles, and the stability was lower than PAANa. This is different from previous CV test results.

In addition, we carried out charge and discharge tests on the cell at different rates, and the results are shown in Figure 2d. The specific discharge capacities of PAANa at 0.1 C, 0.2 C, 0.5 C, 1 C, 2 C, and 3 C are 317 mAh g^{-1}, 305 mAh g^{-1}, 246 mAh g^{-1}, 170 mAh g^{-1}, 96 mAh g^{-1}, and 55 mAh g^{-1}, respectively. At 1 C there is still a capacity

of 200 mAh g^{-1}. The specific discharge capacity of LA133 at 0.1 C, 0.2 C, 0.5 C, 1 C, 2 C, and 3 C is 300 mAh g^{-1}, 292 mAh g^{-1}, 229 mAh g^{-1}, 129 mAh g^{-1}, 61 mAh g^{-1}, and 26 mAh g^{-1}, respectively. Back at 1 C, there is only 153 mAh g−1 capacity. It is obvious that PAANa has a higher capacity at different rates and better recovery at 1C, indicating that it has better cyclic stability.

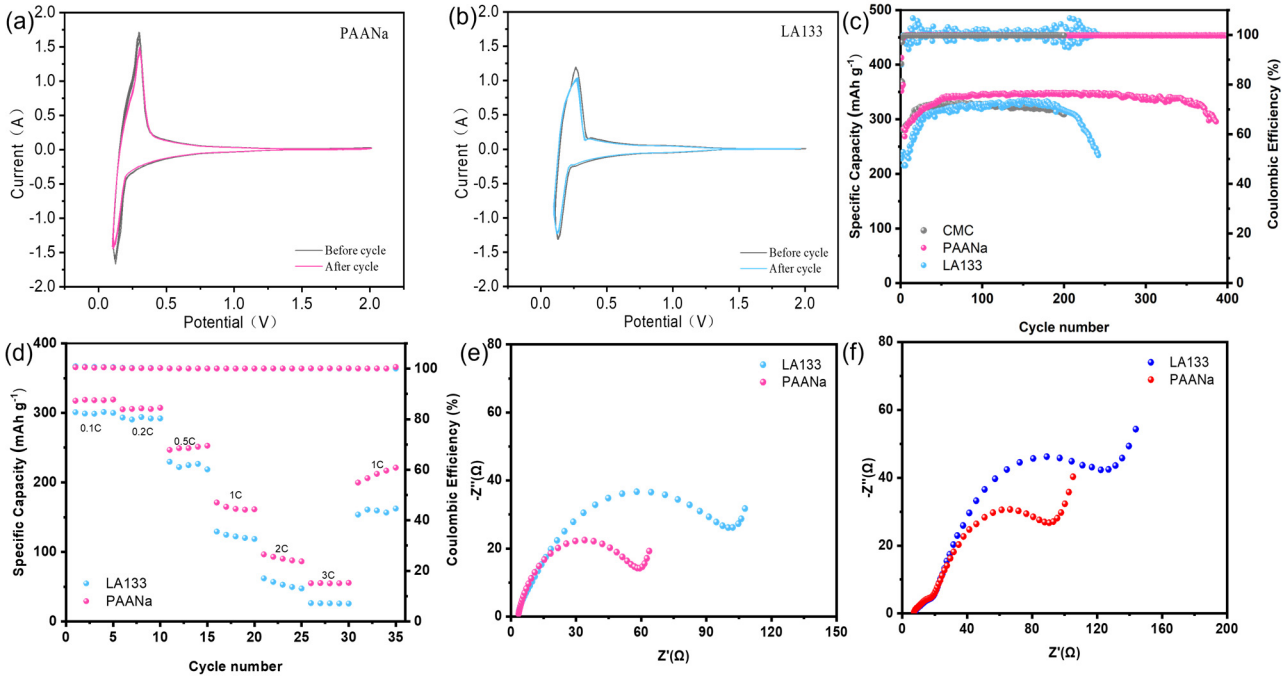

Figure 2. CV curves of (**a**) PAANa and (**b**) LA133. Cycling curves at room temperature (**c**) at 1 C and (**d**) at different rates. EIS (**e**) before and (**f**) after 180 cycles of PAANa and LA133.

The impedance test is performed on the cells after the two binders have just been assembled and after 180 cycles, respectively. The results are shown in Figure 2e,f. It can be intuitively seen that the impedance before and after the battery cycle of PAANa as a binder is significantly smaller than LA133. In addition, the impedance increase in PAANa is slightly smaller than that of LA133 after 180 cycles of the two figures. The higher adhesion strength of PAANa not only facilitates the close contact between the graphite particles and the collector to reduce the interface resistance but also provides better mechanical stability, reduces structural damage during cycling, and maintains a low impedance. It proves that PAANa gives the cell better electrochemical performance.

In order to further understand the changes inside the battery, the cells are separately disassembled after 180 cycles, and the graphite cathode electrode is tested by SEM. In addition, the freshly dried graphite films are also tested by SEM as a control. It can be seen from Figure 3a,d that the graphite inside the newly coated film is a large block. However, although the graphite in the film with PAANa as the binder after cycling is slightly cracked (Figure 3b–d), it is much more complete than the graphite in LA133 (Figure 3e,f). It shows that PAANa has stronger bonding force, which is more conducive to maintaining electrode integrity and electrochemical stability.

After 150 cycles of the two binders, the battery was disassembled and XPS was tested on the surface of lithium metal, respectively, as shown in Figure 4. Compared with the bond intensity, it can be seen that the content of the organic layer in SEI film on lithium metal surface corresponding to PAANa is lower. Interestingly, the graphite electrode had an effect on the surface of the Li metal counter electrode. The high organic layer content of SEI film can increase the Li^+ diffusion impedance, which reduces the cycle stability and service

life of the battery. This is also the reason why the experimentally synthesized PAANa has better battery performance. In addition, Time-of-Flight Secondary Ion Mass Spectrometry (ToF-SIMS) was used to test the structural information of different depths. As shown in Figure 4e, compared with the three-dimensional diagram of C2H2O−, it can be found that the organic layer in SEI film with LA133 as the binder is thicker, which is consistent with the results of XPS.

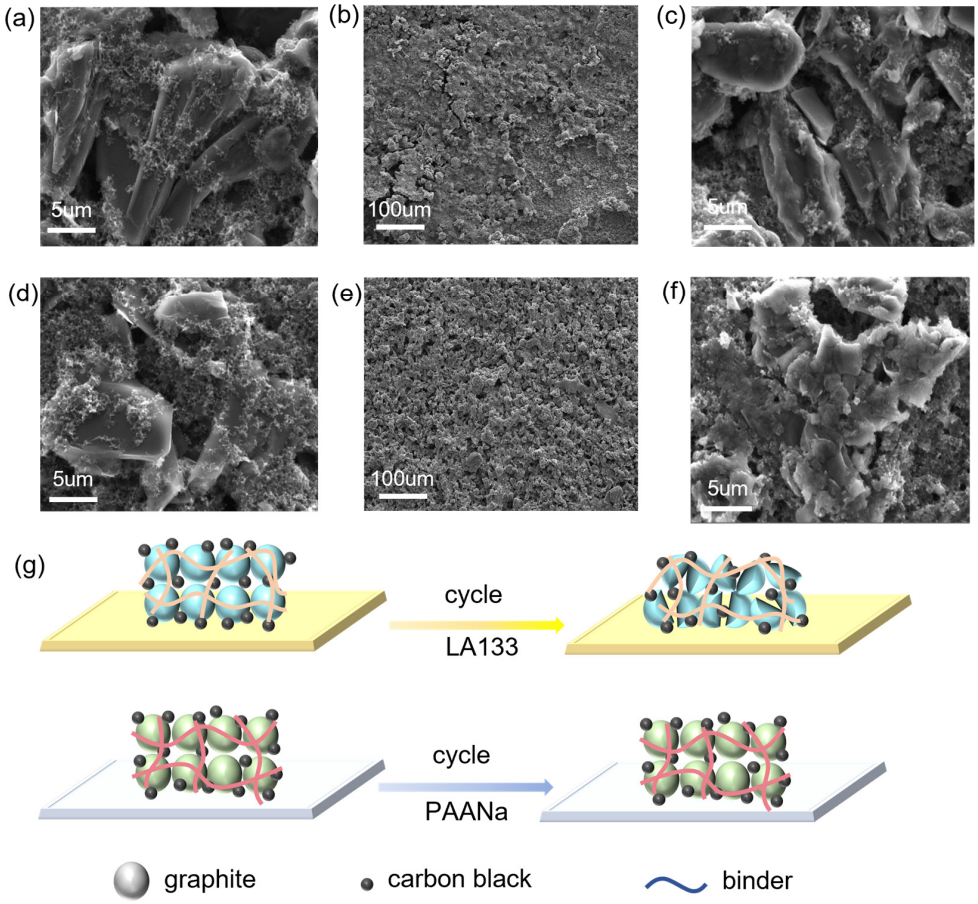

Figure 3. SEM (**a**) fresh, (**b**) high magnification and (**c**) low magnification after 180 cycles of graphite electrodes with PAANa; (**d**) fresh, (**b**,**e**) high magnification and (**f**) low magnification after 180 cycles of graphite electrodes with LA133. (**g**) Diagram of graphite internal circulation change.

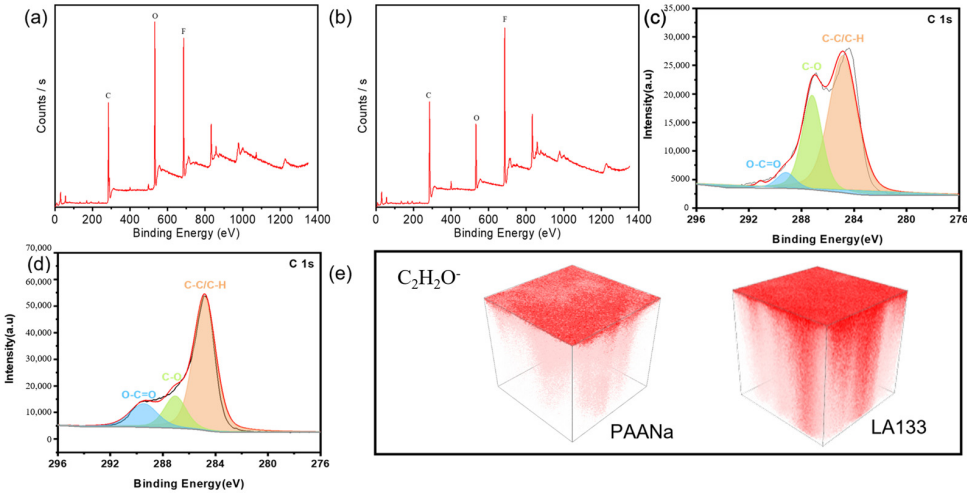

Figure 4. Lithium metal surface XPS of (**a**) PAANa, (**b**) LA133, (**c**) C 1s of PAANa, and (**d**) C 1s of LA133. (**e**) 3D renderings of $C_2H_2O^-$ distribution in the SEI formed on the LMA with PAANa and LA133.

4. Conclusions

We have successfully developed a binder PAANa for graphite electrodes. Graphite expands in volume during charge and discharge (when the lithium is intercalating), and PAANa has sufficient adhesion strength to resist repeated stresses and maintain electrode integrity. It effectively improves the cycle life of the battery and the cycle capacity at high magnification, and it reduces the polarization of the battery. The synthetic path in this experiment has low cost, good electrochemical performance of the sample, and has a certain prospect for industrialization.

Author Contributions: Conceptualization, L.F. and M.L.; validation, F.H.; formal analysis, X.G.; investigation, Y.B.; resources, W.X.; data curation, W.Y.; writing—original draft preparation, W.C.; writing—review and editing, M.L.; visualization, Y.Y. All authors have read and agreed to the published version of the manuscript.

Funding: Financial support from the Natural Science Foundation of China (grant no. 21978231), International Science and Technology Cooperation Program of Shaanxi Province—Key project (grant no. 2022KWZ-08) and the Natural Science Foundation of Jiangsu Province, China (grant no. SBK2020021757). We thank the Instrumental Analysis Center of Xi'an Jiaotong University formaterial characterizations.

Data Availability Statement: Data supporting the findings of this study are available from the corresponding author upon reasonable request.

Conflicts of Interest: The authors declare no conflicts of interest.

References

1. Kang, J.; Kwon, J.Y.; Han, D.Y.; Park, S.; Ryu, J. Customizing polymeric binders for advanced lithium batteries: Design principles and beyond. *Appl. Phys. Rev.* **2024**, *11*. [CrossRef]
2. Deng, L.; Liu, J.-K.; Wang, Z.; Lin, J.-X.; Liu, Y.-X.; Bai, G.-Y.; Zheng, K.-G.; Zhou, Y.; Sun, S.-G.; Li, J.-T. A Formula to Customize Cathode Binder for Lithium Ion Battery. *Adv. Energy Mater.* **2024**, *14*, 2401514. [CrossRef]
3. Hong, S.-B.; Jang, Y.-R.; Kim, H.; Jung, Y.-C.; Shin, G.; Hah, H.J.; Cho, W.; Sun, Y.-K.; Kim, D.-W. Wet-Processable Binder in Composite Cathode for High Energy Density All-Solid-State Lithium Batteries. *Adv. Energy Mater.* **2024**, *14*, 2400802. [CrossRef]
4. Chen, B.; Zhang, Z.; Xiao, M.; Wang, S.; Huang, S.; Han, D.; Meng, Y. Polymeric Binders Used in Lithium Ion Batteries: Actualities, Strategies and Trends. *ChemElectroChem* **2024**, *11*, e202300651. [CrossRef]
5. Jiang, X.; Li, T.; Dong, A.; Yang, D. Synthesis and Evaluation of Poly (Trifluoroethyl Methacrylate) Binders as a Polyvinylidene Fluoride Alternative for Lithium-Ion Batteries. *Energy Technol.* **2024**, *12*, 2400511. [CrossRef]
6. Zhong, S.; Huang, Y.; Zhang, F.; Wang, H.; Liu, P.; Liu, J.; Li, Z.; Li, Y.; Lu, Z. Dextran Sulfate Sodium as Multifunctional Aqueous Binder Stabilizes Spinel $LiMn_2O_4$ for Lithium Ion Batteries. *Adv. Funct. Mater.* **2025**, *35*, 2414602. [CrossRef]
7. Si, M.; Jian, X.; Xie, Y.; Zhou, J.; Jian, W.; Lin, J.; Luo, Y.; Hu, J.; Wang, Y.-J.; Zhang, T.D.; et al. A Highly Damping, Crack-Insensitive and Self-Healable Binder for Lithium-Sulfur Battery by Tailoring the Viscoelastic Behavior. *Adv. Energy Mater.* **2024**, *14*, 2303991. [CrossRef]
8. Wang, W.; Hua, L.; Zhang, Y.; Wang, G.; Li, C. A Conductive Binder Based on Mesoscopic Interpenetration with Polysulfides Capturing Skeleton and Redox Intermediates Network for Lithium Sulfur Batteries. *Angew. Chem. Int. Ed.* **2024**, *63*, e202405920. [CrossRef] [PubMed]
9. Patra, A.; Matsumi, N. Densely Imidazolium Functionalized Water Soluble Poly(Ionic Liquid) Binder for Enhanced Performance of Carbon Anode in Lithium/Sodium-Ion Batteries. *Adv. Energy Mater.* **2025**, *15*, 2403071. [CrossRef]
10. Su, Z.; Li, G.; Zhang, J. Coaxial Nanofiber Binders Integrating Thin and Robust Sulfide Solid Electrolytes for High-Performance All-Solid-State Lithium Battery. *Adv. Funct. Mater.* **2025**, *35*, 2415409. [CrossRef]
11. Trivedi, S.; Pamidi, V.; Bautista, S.P.; Shamsudin, F.N.A.; Weil, M.; Barpanda, P.; Bresser, D.; Fichtner, M. Water-Soluble Inorganic Binders for Lithium-Ion and Sodium-Ion Batteries (Adv. Energy Mater. 9/2024). *Adv. Energy Mater.* **2024**, *14*, 2470041. [CrossRef]
12. Gupta, A.; Badam, R.; Mantripragada, B.S.; Mishra, S.N.; Matsumi, N. Ultra-Durability and Reversible Capacity of Silicon Anodes with Crosslinked Poly-BIAN Binder in Lithium-Ion Secondary Batteries for Sturdy Performance. *Adv. Sustain. Syst.* **2025**, *9*, 2400263. [CrossRef]

13. Yang, K.; Chen, K.; Zhang, X.; Gao, S.; Sun, J.; Gong, J.; Chai, J.; Zheng, Y.; Liu, Z.; Wang, H. Exploring Phenolphthalein Polyarylethers as High-Performance Alternative Binders for High-Voltage Cathodes in Lithium-Ion Batteries. *Small* **2024**, *20*, 2403993. [CrossRef] [PubMed]
14. Dou, W.; Zheng, M.; Zhang, W.; Liu, T.; Wang, F.; Wan, G.; Liu, Y.; Tao, X. Review on the Binders for Sustainable High-Energy-Density Lithium Ion Batteries: Status, Solutions, and Prospects. *Adv. Funct. Mater.* **2023**, *33*, 2305161. [CrossRef]
15. Zhang, S.S. Impact of Binder Content and Type on the Electrochemical Performance of Silicon Anode Materials. *ChemPhysChem* **2024**, *25*, e202400570. [CrossRef] [PubMed]
16. Wang, W.; Yue, X.; Meng, J.; Wang, X.; Zhou, Y.; Wang, Q.; Fu, Z. Comparative Study of Water-Based LA133 and CMC/SBR Binders for Sulfur Cathode in Advanced Lithium–Sulfur Batteries. *J. Phys. Chem. C* **2019**, *123*, 250–257. [CrossRef]
17. Tatara, R.; Umezawa, T.; Kubota, K.; Horiba, T.; Takaishi, R.; Hida, K.; Matsuyama, T.; Yasuno, S.; Komaba, S. Effect of Substituted Styrene-Butadiene Rubber Binders on the Stability of 4.5 V-Charged LiCoO2 Electrode. *ChemElectroChem* **2021**, *8*, 4345–4352. [CrossRef]
18. Müllner, S.; Michlik, T.; Reichel, M.; Held, T.; Moos, R.; Roth, C. Effect of Water-Soluble CMC/SBR Binder Ratios on Si-rGO Composites Using µm- and nm-Sized Silicon as Anode Materials for Lithium-Ion Batteries. *Batteries* **2023**, *9*, 248. [CrossRef]
19. Jin, B.; Li, Y.; Qian, J.; Zhan, X.; Zhang, Q. Environmentally Friendly Binders for Lithium-Sulfur Batteries. *ChemElectroChem* **2020**, *7*, 4158–4176. [CrossRef]
20. Oli, N.; Choudhary, S.; Weiner, B.R.; Morell, G.; Katiyar, R.S. Comparative Investigation of Water-Based CMC and LA133 Binders for CuO Anodes in High-Performance Lithium-Ion Batteries. *Molecules* **2024**, *29*, 4114. [CrossRef] [PubMed]